JOURNAL OF SOLID STATE CHEMISTRY 83, 340–349 (1989)

F^+ Center as a Paramagnetic Probe in the EPR Investigation of Barium Hexaaluminate Phases I and II and Barium–Lanthanum Hexaaluminate Ceramics

T. GBEHI, D. GOURIER,* J. THERY, AND D. VIVIEN

Laboratoire de Chimie Appliquée de l'état solide, UA-CNRS 302
11, rue Pierre et Marie Curie, 75231 Paris Cedex 05, France

Received January 31, 1989; in revised form July 18, 1989

An X-ray-induced F^+ center is used as a paramagnetic probe to study sintered powders of barium hexaaluminates phases I and II (referred to as $Ba(\Phi_I)$ and $Ba(\Phi_{II})$) and mixed barium–lanthanum hexaaluminate (referred to as BLA). This F^+ center was previously shown to exist only in β-alumina-type mirror planes containing interstitial oxygen ions as charge-compensating defects, so that its study yields information about the local structure of this type of mirror plane. By comparison of the EPR spectra of $Ba(\Phi_I)$ and $Ba(\Phi_{II})$ it is shown that the latter contains only one type of F^+ center with a reduced hf interaction. This indicates that there is only one type of mirror plane containing interstitial oxygen in $Ba(\Phi_{II})$ and that the separation between spinel blocks is larger in $Ba(\Phi_{II})$ than in $Ba(\Phi_I)$. This result agrees with models proposed by other authors for barium–lead hexaaluminate and barium hexagallate. Investigation of the F^+ center in mixed barium–lanthanum hexaaluminate ceramics clearly supports the hypothesis of segregation of Ba^{2+} ions in β-alumina-type mirror planes. It is also shown that the structure of these planes is very similar to that of $Ba(\Phi_{II})$ defect planes.

(I) Introduction

Hexaaluminates cover two similar and well-known classes of compounds. The first class of the general formula $MAl_{11}O_{17}$ (M = Na^+, K^+, Ag^+, etc.) encompasses β-alumina (β)-type structures (*1*). The second class includes the compounds $MAl_{12}O_{19}$ (M = Pb^{2+}, Ca^{2+}, Sr^{2+}, etc.), "$LnAl_{11}O_{18}$," or $LnMAl_{11}O_{19}$ (Ln = La^{3+}, Nd^{3+}, . . . , M = Mg^{2+}, Ni^{2+}, Co^{2+}, . . .) and is related to magnetoplumbite (MP) structure (*2*). Both β and MP structures belong to space group $P6_3/mmc$. Their unit cell is formed by stacks of spinel-like blocks separated by two mirror planes containing the large cation. The two structures differ only by their mirror planes (Fig. 1).

According to the above structural classification, hexagonal barium aluminate was first considered isostructural with $CaAl_{12}O_{19}$ and $SrAl_{12}O_{19}$ having MP structure (*3*). However, several investigations in the last 10 years have shown that the ideal composition $BaAl_{12}O_{19}$ does not exist (*4*). The phase relations established by Kimura *et al.* (*5*) on sintered compounds obtained at high temperature (about 1600°C) have clarified the existence of two different phases labeled phase I and phase II (hereafter referred to as $Ba(\Phi_I)$ and $Ba(\Phi_{II})$) having respectively the approximate compositions

* To whom correspondence should be addressed.

0022-4596/89 $3.00

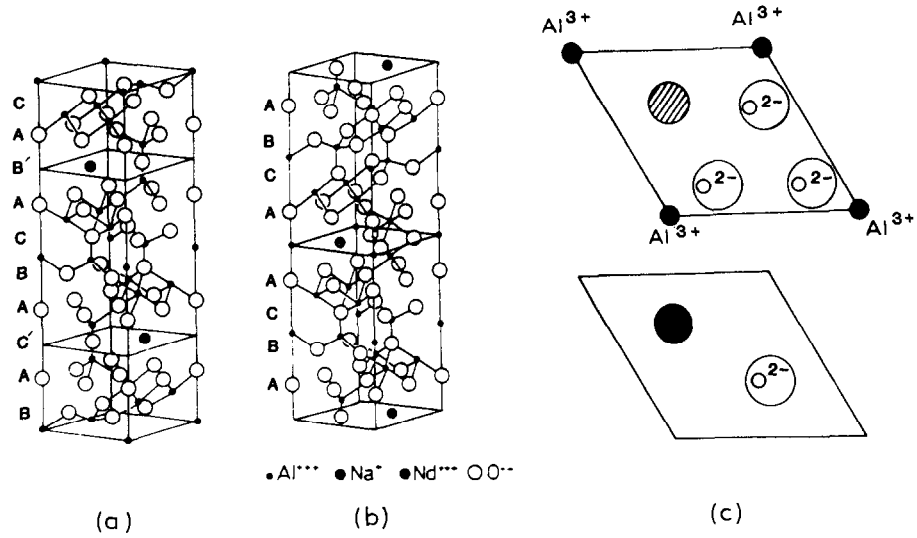

FIG. 1. (a) Unit cell of ideal β-alumina compound with formula $NaAl_{11}O_{17}$ and (b) of a mixed β-alumina–magnetoplumbite compound (SLnA). (c) Ideal distribution of ions in mirror planes of $NaAl_{11}O_{17}$ (β-alumina) and $LaMgAl_{11}O_{19}$) (magnetoplumbite).

$0.8BaO, 6Al_2O_3$ and $1.3BaO, 6Al_2O_3$. The lattice parameters are $\mathbf{a_I} = 0.5588$ nm, $\mathbf{c_I} = 2.270$ nm for $Ba(\Phi_I)$ and $\mathbf{a_{II}} = 0.5600$ nm, $\mathbf{c_{II}} = 2.291$ nm for $Ba(\Phi_{II})$. Within the range of these two well-defined compositions, the observation of splitting or broadening of some reflections in X-ray diffraction patterns demonstrated the presence of a mixture of phases I and II (hereafter referred to as $Ba(\Phi_I + \Phi_{II})$). Radiocrystallographic studies on $Ba(\Phi_I)$ single crystals established that this phase is of β-alumina type (*6, 7*). Although mixed barium–lead hexaaluminate phase II (hereafter referred to as $BaPb(\Phi_{II})$) single crystals have been synthesized by Iyi *et al.* (*8–10*), pure $Ba(\Phi_{II})$ crystals have not yet been obtained, and many studies by electron microscopy and X-ray diffraction techniques have been devoted to its structure (*8, 11–14*). Increase in the **c** parameter of $Ba(\Phi_{II})$ compared to that of $Ba(\Phi_I)$ is due to an excess of barium ions which has been explained by different mechanisms:

(i) Alternating of mirror planes of Φ_I type with barium-rich mirror planes (*8, 12, 13*).

(ii) Only one type of mirror plane containing the excess barium (*11, 14*).

(iii) A third mechanism proposed by Iyi *et al.* (*9, 10*) for $BaPb(\Phi_{II})$ that consists of perfect cells ($Ba_{2.0}Al_{22.0}O_{34.0}$) and defect cells ($(BaPb)_{3.0}Al_{20.0}O_{35.0}$) in a 2:1 ratio. The defect cell was shown to contain a Ba or Pb ion in the center of the spinel block.

(iv) Another model was recently proposed by Wagner and O'Keeffe (*15*) for barium hexagallate of phase II type, which bears some similarities with the preceding one except that there are no Ba ions in the center of the spinel blocks. In this model, two Ba ions are positioned in the oxygen layers directly on either side of an anti-BR (aBR) site in alternating mirror planes in one of every three unit cells proposed by Iyi *et al.* (*9, 10*).

In a previous paper (*16*) we reported the synthesis by solid-state reaction and the characterization by Nd^{3+} spectroscopy of mixed barium–lanthanide hexaaluminate compounds (B*Ln*A) with approximate composition $x/2BaO, x/6Ln_2O_3, 6Al_2O_3$ ($1.2 < x < 1.5$; *Ln* = La, Nd). Its structure was

shown to be of S*Ln*A type (mixed sodium–lanthanide hexaaluminate) (*17*). In this type of compound, Ba^{2+} and Ln^{3+} ions are thought to be in two kinds of mirror planes of β and MP types, respectively. In B*Ln*A, which is obtained as a pure phase only in the powder state, this assumption is based on the observation of odd (00*L*) reflections in X-ray diffraction patterns and of well-defined compositions for Ba^{2+} and Ln^{3+} cations.

We report in this work the EPR study of various barium hexaaluminates using a paramagnetic probe. It is now well-established that X-ray irradiation of β-aluminate single crystals generates paramagnetic defects, essentially F^+ centers (a single electron trapped at a vacant oxygen site) and oxygen centers localized in the mirror planes. These have been observed in sodium, potassium, and lithium β-alumina (*18–20*). The F^+ center lies in a site sharing two tetrahedral Al^{3+} sites, the two possible oxygen sites being O(5) and the interstitial *m*O positions.

We recently observed this defect in Ba(Φ_1) single crystals. More precisely we distinguished two different centers, labeled $(F^+)_\alpha$ and $(F^+)_\beta$. The results, including the defect structures and their thermal stability studied by optical absorption, thermally stimulated luminescence, and EPR, have been reported separately (*21*). The behavior of hexaaluminates with MP structure is significantly different. Investigation of $LaMgAl_{11}O_{19}$ single crystals (*22*) have shown that the X-ray-induced defects are located in the spinel blocks and are mainly holes trapped at cationic defects (V-type centers). We also observed similar defects in other MP compounds such as $CaAl_{12}O_{19}$ and $SrAl_{12}O_{19}$ ceramics (*23*).

The F^+ centers in mirror planes of β-alumina thus constitute "fingerprints" for the identification of β-alumina structure. Moreover the potential which traps the electron is essentially spherical, which means that the electronic state can be considered hydrogenoid-like. Consequently the EPR spectrum is not sensitive to the orientation of the magnetic field B_0 with respect to the crystallographic axes and should be easily observable in powders and ceramics.

With these considerations in mind, we performed a systematic EPR study of sintered powders of barium hexaaluminates with starting compositions xBaO, $6Al_2O_3$ ($0.8 \leq x \leq 1.3$) and of BLA compound with compositions x/2BaO, x/6La_2O_3, $6Al_2O_3$ ($1.2 \leq x \leq 1.55$). The purpose was to obtain additional information concerning the local structure of mirror planes.

(II) Experimental

The sintered samples (about 2 g in weight) were obtained at high temperature (1600°C) by usual solid-state reaction techniques. The starting materials were $BaCO_3$, Al_2O_3, and La_2O_3 in appropriate proportions. The phases obtained after heating were characterized by X-ray powder diffraction. We prepared the following compositions: xBaO, $6Al_2O_3$ (x = 0.80, 0.85, 0.90, 0.95, 1.00, 1.05, 1.10, 1.15, 1.20, 1.25, 1.30) and x/2BaO, x/6La_2O_3, $6Al_2O_3$ (x = 1.25, 1.30, 1.40, 1.50, 1.55). A reference sample was also prepared by grinding single crystals of pure Ba(Φ_1) with x = 0.75, grown by zone melting in an arc image furnace (*24*).

Irradiation of the samples was performed at room temperature using 40-kV, 20-mA X-rays from a copper target tube. The beam consists of unfiltered X radiations of $K\alpha$ (0.154 nm) and $K\beta$ (0.139 nm) emissions of copper. All the samples were irradiated for 16 hr. The irradiated samples were studied in slices or powder form, the results being the same in both cases.

EPR spectra were recorded at room temperature using a Bruker ER 220 D spectrometer working at X-band and equipped with a gaussmeter and a frequency meter.

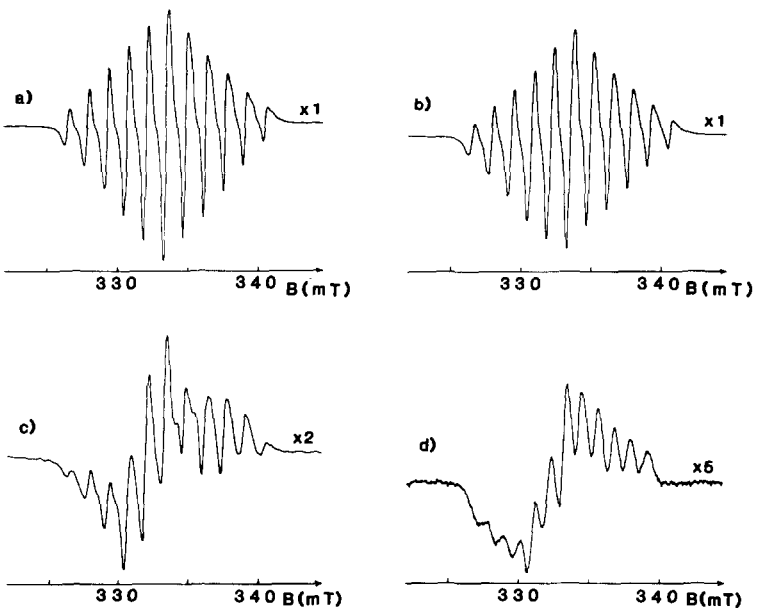

FIG. 2. EPR spectra recorded at room temperature of barium aluminate ceramics with compositions xBaO, $6Al_2O_3$. Irradiation time: 16 hr. Microwave power: 10 mW. (a) $x = 0.80$; Ba(Φ_I). (b) $x = 1.00$; Ba($\Phi_I + \Phi_{II}$). (c) $x = 1.15$; Ba($\Phi_I + \Phi_{II}$). (d) $x = 1.30$; Ba(Φ_{II}).

(III) Results

Figure 2a shows the EPR spectrum, recorded at room temperature and 10 mW microwave power, of a sample of pure Ba(Φ_I) with composition $x = 0.80$. It exhibits the 11-line hyperfine pattern of the F^+ center typical of β-alumina phases. The line intensities are in the ratios 1:2:3:4:5:6:5:4:3:2:1, indicating that the unpaired electron at the vacant oxygen site of the mirror plane interacts with two equivalent ^{27}Al nuclei with spin 5/2. This EPR spectrum is very similar to that of Ba(Φ_I) single crystals (*21*), except that the anisotropy cannot be observed since we are dealing with a polycrystalline sample. The good spectral resolution is due to the very small anisotropy of the hf interaction, which amounts to $b = 0.1$ MHz, a value much smaller than that of the dipolar contribution $b_{dip} = 4.2$ MHz expected from the classical point dipole–dipole interaction (*21*). As a result the hf interaction measured in the powder sample $\langle A \rangle_I = 1.40$ mT is close to the values $a = 1.49$ and 1.45 mT measured, respectively, for the isotropic interaction of $(F^+)_\alpha$ and $(F^+)_\beta$ centers in Ba(Φ_I) single crystals. The experimental g value $\langle g \rangle_I = 2.0035$ measured in powder samples is also very close to the mean value $g_{iso} = (g_x + g_y + g_z)/3 = 2.0033$ obtained for $(F^+)_\alpha$ and $(F^+)_\beta$ centers in Ba(Φ_I) crystals. Control experiment showed that the EPR spectrum of ground single crystals of Ba(Φ_I) is rigorously identical with that of the powder synthesized by solid-state reactions.

The EPR spectrum of a pure Ba(Φ_{II}) powder (corresponding to $x = 1.3$), recorded under the same conditions as that of Ba(Φ_I), is shown in Fig. 2d. It also exhibits the 11-line hf pattern which immediately indicates that the structure of Ba(Φ_{II}) is of β-alumina type. For a magnetoplumbite structure we expect only a broad anisotropic line due to V-type centers located in

spinel blocks of the structure (*22*). It should be noted, however, that the EPR spectrum is not identical with that of $Ba(\Phi_I)$, which reveals some differences in the structure of the mirror planes. The spectrum is slightly disymmetrical, which might be due to a larger anisotropy of the g factor and (or) the hf interaction. The experimental parameters are $\langle g\rangle_{II} = 2.0057$ and $\langle A\rangle_{II} = 1.12$ mT, the latter being significantly smaller than the value measured in $Ba(\Phi_I)$ powder.

Another difference with $Ba(\Phi_I)$ concerns the EPR intensity and the saturation behavior. Figure 3 shows the saturation plots at room temperature for two equal amounts of $Ba(\Phi_I)$ ($x = 0.8$) and $Ba(\Phi_{II})$ ($x = 1.3$) powders. The striking feature is that the F^+ center saturates more readily in $Ba(\Phi_{II})$ than in $Ba(\Phi_I)$. In the former case, saturation occurs at a moderate microwave power $P \approx 20$ mW, while in the latter the maximum intensity is not yet reached at $P \approx 200$ mW. This indicates that the spin lattice relaxation time T_1 of F^+ centers is longer in $Ba(\Phi_{II})$ than in $Ba(\Phi_I)$. Furthermore the saturation plot of $Ba(\Phi_{II})$ exhibits a decreasing intensity at $P > 20$ mW, which shows that the EPR lines are homogeneously broadened. For a magnetic resonance absorption Y with Lorentzian lineshape, the first derivative Y' depends on the spin lattice relaxation time T_1, on the spin–spin relaxation time T_2, and on the microwave amplitude H_1. Below the saturation level, i.e., when $H_1^2\gamma^2T_1T_2 \ll 1$, Y' does not depend on T_1 and it varies linearly with H_1,

$$Y' = \frac{16}{3^{3/2}} \frac{(B - B_0)\gamma T_2 y_m H_1}{[1 + (B - B_0)^2\gamma^2 T_2^2]^2}, \quad (1)$$

where y_m is the amplitude below saturation. Knowing that the incident power is proportional to H_1^2 and with the two spectra having very similar linewidths $\Delta H_{pp} = 2/(3^{1/2}\gamma T_2)$, the ratio of the slopes of the curves giving the peak-to-peak amplitude A as a function of $P^{1/2}$ below saturation depends only on y_m, which is proportional to the concentration of F^+ centers:

$$\frac{dA_I/dH_1}{dA_{II}/dH_1} = \frac{(y_m)_I}{(y_m)_{II}} = \frac{[F^+]_I}{[F^+]_{II}}. \quad (2)$$

Saturation plots of Fig. 3 give $[F^+]_I/[F^+]_{II} \approx 3$. Comparison of the EPR spectra of $Ba(\Phi_I)$ powder with that of $Ba(\Phi_I)$ single crystal shows that the concentration of F^+ centers is of the order of one F^+ center for 10^4 unit cells. Consequently the concentration of F^+ centers in phases I and II are both very small, and if they are supposed to be randomly distributed in the matrices, they cannot interact. However, a significant shortening of T_1 can occur if there is some defect clustering, as shown for optical bleaching experiments of F centers in KCl (*25*). We thus propose that F^+ centers are partially clustered in $Ba(\Phi_I)$ and more statistically distributed to $Ba(\Phi_{II})$. Recently X-ray and electron diffuse scattering in $Ba(\Phi_I)$ single crystals gave evidence of local ordering of Ba^{2+} and vacancies (*24*). The short-

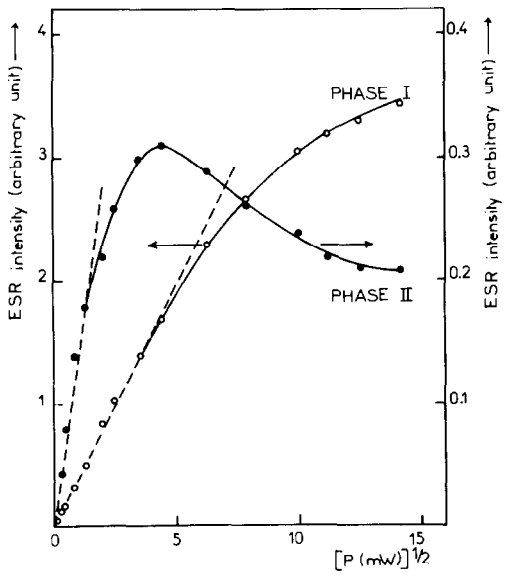

FIG. 3. Variation of the peak-to-peak EPR amplitude at room temperature versus the square root of the microwave power P for $Ba(\Phi_I)$ ($x = 0.80$) and $Ba(\Phi_{II})$ ($x = 1.3$) ceramics.

range order covers about 60 Å and the ordered domains are limited by zones which contain barium vacancies, interstitial oxygen ions, and barium clusters. Moreover we recently showed that F^+ centers are most probably located at sites normally occupied by interstitial oxygen ions (*21*). In view of these results, short T_1 could likely be due to a partial clustering of F^+ centers at the boundary of ordered domains in $Ba(\Phi_I)$. On the contrary, the long T_1 of F^+ centers in $Ba(\Phi_{II})$ reflects a random distribution of these defects which could result from the lack of short-range ordering.

We also investigated F^+ centers in barium hexaaluminate powders with compositions in the range $0.8 < x < 1.3$ containing $Ba(\Phi_I + \Phi_{II})$. The EPR spectra are dominated in this case by F^+ centers of $Ba(\Phi_I)$ since this phase contains a higher concentration of defects than $Ba(\Phi_{II})$. Two representative spectra are shown in Figs. 2b and 2c. In the range $0.8 \leq x \leq 1.05$ the spectra are completely independent of the composition (except for their intensity) and are typical of $Ba(\Phi_I)$. In the range $1.05 \leq x \leq 1.20$ a slight anisotropy appears at the low field side, due to the contribution of the F^+ center of $Ba(\Phi_{II})$. However, the F^+ center of $Ba(\Phi_I)$ is still predominant and the hf parameter $\langle A \rangle$ is that of $Ba(\Phi_I)$ as shown in Fig. 4. In the range $1.25 \leq x \leq 1.30$ the lineshape, g, and hf parameters are those of $Ba(\Phi_{II})$. The evolution of $\langle A \rangle$ with composition is shown in Fig. 4. The hf parameter does not vary in the composition range $0.8 < x < 1.2$, which indicates that $Ba(\Phi_I)$ has a well-defined composition and that there is no intermediate phase between $Ba(\Phi_I)$ and $Ba(\Phi_{II})$.

Another interesting behavior concerns the evolution with x of the concentration of F^+ centers in $Ba(\Phi_I)$. This measure is possible in the range $0.8 \leq x \leq 1.10$ and at high microwave power because these centers almost dominate the EPR spectrum. For example at $P = 100$ mW the EPR intensity of

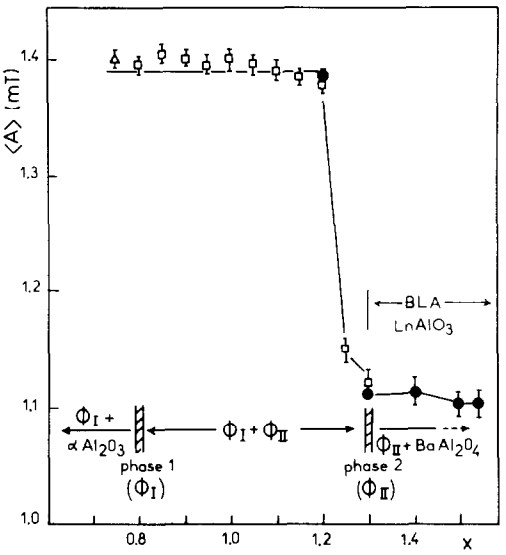

FIG. 4. Variation of the hf parameter $\langle A \rangle$ of F^+ center according to the barium content x in xBaO, $6Al_2O_3$ (rectangles) and in $x/2$BaO, $x/6La_2O_3$, $6Al_2O_3$ (solid circles) powders. The triangle represents the value measured in ground $Ba(\Phi_I)$ single crystals.

F^+ in $Ba(\Phi_I)$ is 13 times that measured in $Ba(\Phi_{II})(x = 1.3)$. In order to obtain this information, we need the variation with x of $P_{\Phi I}$, which is the proportion of phase I in the powder. $P_{\Phi I}$ can be determined from powder X-ray diffraction patterns by monitoring the diffraction peak 20.14 occurring at $d = 0.1346$ nm in $Ba(\Phi_I)$ and $d = 0.1355$ nm in $Ba(\Phi_{II})$. Figure 5 shows the variation with x of the quantity $P_{\Phi I} = I_{\Phi I}/(I_{\Phi I} + I_{\Phi II})$ where $I_{\Phi I}$ and $I_{\Phi II}$ represent the intensity of the 20.14 diffraction peak for $Ba(\Phi_I)$ and $Ba(\Phi_{II})$, respectively. This figure also shows the variation of the quantity $C_{\Phi I} = I_{EPR}/P_{\Phi I}$, which is proportional to the concentration of F^+ centers in $Ba(\Phi_I)$. I_{EPR} is the intensity of the EPR transition $m_I = 1$. We choose this transition instead of the central one ($m_I = 0$) because the latter is generally superimposed on the EPR line of O^- centers, an extra signal well-characterized in our study of $Ba(\Phi_I)$ single crystals (*21*). $C_{\Phi I}$ is in arbitrary units and the value

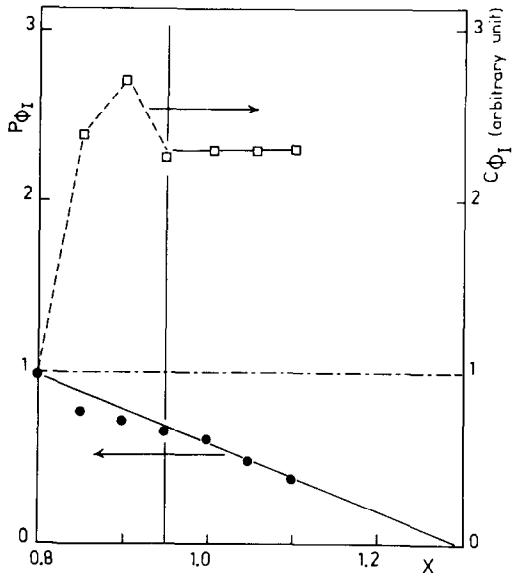

FIG. 5. Variation of the proportion $P_{\Phi I}$ of Ba(Φ_I) and the F^+ concentration $C_{\Phi I}$ (arbitrary unit) in Ba(Φ_I) according to the x value in barium aluminates with starting composition xBaO, $6Al_2O_3$.

$C_{\Phi I} = 1$ has been taken for the pure Ba(Φ_I) phase ($x = 0.8$). For a concentration of F^+ centers in Ba(Φ_I) independent of x, we expect $C_{\Phi I} = 1$ in all the composition range. Surprisingly, we observe a strong increase in $C_{\Phi I}$ by a factor 2.7 in the range $0.80 < x \leq 0.90$, and $C_{\Phi I}$ is constant for $x \geq 0.95$. We have not yet found a satisfactory explanation for this behavior. The fact that the hf parameter is constant shows that the increase in F^+ concentration is not due to a variation of the composition of the mirror planes (see Section IV). It is, however, possible that a change with x of the size of the ordered domains modifies the number of available sites for the oxygen vacancies.

Figure 6 shows the EPR spectra of BLA powders with compositions $x = 1.4$. It is very similar in shape to that of Ba(Φ_{II}), with the same $\langle g \rangle$ and $\langle A \rangle$ parameters. Since this F^+ center can be considered as a "fingerprint" of the β structure, its occurrence in BLA phase indicates that the local environment of the defect in the mirror plane is of β-alumina type. The hf parameters of BLA compounds with starting compositions in the range $1.2 \geq x \geq 1.55$ are reported in Fig. 4. It is noteworthy that $\langle A \rangle$ in BLA follows the variation obtained for Ba($\Phi_I + \Phi_{II}$) mixtures in the range $x = 1.2$ to $x = 1.3$. The results show that barium planes of BLA with $x > 1.3$ have barium composition very similar to Ba(Φ_{II}). On the contrary the β-alumina-type mirror plane of BLA with $x = 1.2$ seems to be very similar to that of Ba(Φ_I) since their EPR spectra are almost identical. It might also be possible that this F^+ center in BLA for $x = 1.2$ arises from traces of Ba(Φ_I) phase in addition to BLA. However, X-ray diffraction on this BLA does not reveal the presence of any additional phase (except α-Al_2O_3) while the associated EPR spectrum is intense.

(IV) Discussion

It is now well established that the 11-line hf pattern of F^+ centers is a fingerprint of the β-alumina phase (*18–22*). Recent work has shown that the F^+ center is not produced in either stoichiometric β-alumina (*26*) or β''-alumina (*27*). This defect thus exists only in β-alumina having interstitial oxygen ions. This behavior leads us to interpret the defect as being an electron trapped

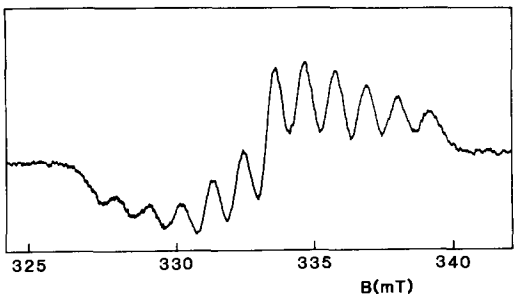

FIG. 6. EPR spectrum at room temperature of a mixed barium–lanthanum aluminate ceramics with starting composition x/2BaO, x/6La_2O_3, $6Al_2O_3$ ($x = 1.4$). Irradiation time: 16 hr. Microwave power: 10 mW.

at the site of an interstitial oxygen and delocalized on the alumium ions of two adjacent Frenkel defects (*21*). We may thus use this defect to identify mirror planes possessing interstitial oxygen ions.

The second point is that the hf interaction is sensitive to the local structure of the mirror plane, more precisely to the distance between aluminum ions of the two Frenkel defects. The dramatic change of the hf parameter, namely $\langle A\rangle_{\mathrm{I}} = 1.40$ mT and $\langle A\rangle_{\mathrm{II}} = 1.12$ mT in $Ba(\Phi_{\mathrm{I}})$ and $Ba(\Phi_{\mathrm{II}})$, respectively, indicates that the mirror planes do not have the same composition. In Section III, we pointed out that the experimental value of $\langle A\rangle_{\mathrm{I}}$ is very close to the isotropic interaction a_{I} measured in $Ba(\Phi_{\mathrm{I}})$ single crystals. The value a is related to the square of the wave function $|\Psi(0)|^2$ of the unpaired electron at the ^{27}Al nucleus by

$$a = \frac{8\pi}{3} g\beta g_{\mathrm{N}}\beta_{\mathrm{N}}|\Psi(0)|^2. \qquad (3)$$

In the point ion theory of Gourary and Adrian (*28*) for F centers, the wave function Ψ is made of a smoothly varying envelop function Ψ_{F} centered at the vacancy, which is orthogonalized to the ion core orbitals Ψ_i of the two Al^{3+} ions. Gourary and Adrian have shown that the result is equivalent to replacing $|\Psi(0)|^2$ in Eq. 3 by $A_R|\Psi_{\mathrm{F}}(R)|^2$ where A_{R} is an amplification factor for the nucleus at distance R from the vacancy center. A_R is almost independent of distance (*29*) and the envelope function was found to vary as R^{-3} so that we may write

$$\frac{\langle A\rangle_{\mathrm{I}}}{\langle A\rangle_{\mathrm{II}}} \approx \frac{a_{\mathrm{I}}}{a_{\mathrm{II}}} \approx \frac{|\Psi_{\mathrm{F}}(R_{\mathrm{I}})|^2}{|\Psi_{\mathrm{F}}(R_{\mathrm{II}})|^2} \approx \left(\frac{R_{\mathrm{II}}}{R_{\mathrm{I}}}\right)^3, \qquad (4)$$

where R_{I} and R_{II} represent the "oxygen vacancy"–Al^{3+} distances in $Ba(\Phi_{\mathrm{I}})$ and $Ba(\Phi_{\mathrm{II}})$. From the experimental values of $\langle A\rangle_{\mathrm{I}}$ and $\langle A\rangle_{\mathrm{II}}$ we get $R_{\mathrm{II}}/R_{\mathrm{I}} = 1.08$. EPR results show that the separation between spinel blocks is larger in $Ba(\Phi_{\mathrm{II}})$ than in $Ba(\Phi_{\mathrm{I}})$. Several workers observed that an increasing cation concentration in mirror planes results in decreasing separation between spinel blocks (*30*). This might indicate that the barium concentration in mirror planes (containing interstitial oxygen) of $Ba(\Phi_{\mathrm{II}})$ is smaller than that in $Ba(\Phi_{\mathrm{I}})$.

In Section I, we considered four different mechanisms invoked to explain the excess barium ions. The existence of only one type of F^+ center in $Ba(\Phi_{\mathrm{II}})$ with small hf interaction shows that this compound possesses only one type of mirror plane with defect oxygen, also characterized by a reduced barium content (with respect to $Ba(\Phi_{\mathrm{I}})$). If $Ba(\Phi_{\mathrm{II}})$ contains two types of mirror planes, the other one should be "ideal," i.e., without defect oxygen. This ideal mirror plane is similar to that of stoichiometric β-alumina and is thus expected to exhibit no F^+ centers. These considerations allow us to eliminate mechanisms (i) and (ii) because the former should imply the existence of two different F^+ centers, one of them being of $Ba(\Phi_{\mathrm{I}})$ type. Mechanism (ii) would be characterized by only one type of F^+ center, but since the barium concentration in mirror planes of $Ba(\Phi_{\mathrm{II}})$ should be higher than that in $Ba(\Phi_{\mathrm{I}})$, the former should exhibit a larger hf coupling than the latter, which is not the case. Models (iii) and (iv) differ by the site of the spinel blocks containing excess barium, but they are similar in the sense that they both postulate the existence of two different types of mirror planes, one having only one barium ion and no defect oxygen ion. This ideal plane should be undetectable by EPR. The other plane, which contains interstitial oxygen ions and a reduced barium content, has a structure compatible with the existence of F^+ centers with reduced hf interaction detected by EPR. The F^+ concentration, which is smaller in $Ba(\Phi_{\mathrm{II}})$ than in $Ba(\Phi_{\mathrm{I}})$, also agrees with the existence of these ideal planes. It should be noted however that paramagnetic centers are only sensitive to short-range interactions, which implies that

we cannot determine the localization of the excess barium.

This discussion is also valid for BLA compound. The existence of F^+ centers clearly demonstrates that barium ions are located in β-alumina-type mirror planes. Moreover the complete similitude of the EPR spectra of BLA and Ba(Φ_{II}) for $x \geq 1.3$ shows that lanthanum and barium ions are located in different mirror planes so that the EPR spectrum is not sensitive to the presence of La^{3+} in the lattice. A localization of La^{3+} and Ba^{2+} ions in the same plane should be detectable on the EPR spectrum of the F^+ center, which is not the case. The hypothesis of a segregation of Ba^{2+} and La^{3+} ions in different mirror planes of β and MP types, respectively (*16*), is thus fully supported. This similitude also indicates that the β-alumina mirror planes of BLA ($x > 1.3$) are of Φ_{II} type and not of Φ_I type, which seems to indicate that the barium content of these planes in BLA is smaller than that of Ba(Φ_I). The hf parameter $\langle A \rangle$ does not depend on x in this composition range, which indicates that BLA has a well-defined barium content. Thus for $x \geq 1.3$, a phase separation should occur leading to BLA and another phase identified as $LnAlO_3$ (*16*). The similitude of BLA and Ba(Φ_{II}) F^+ centers also indicates that the compensation mechanisms for the excess barium are probably identical in these two compounds. The case of BLA ($x = 1.2$) is more problematic since we are not certain whether the hf parameter $\langle A \rangle = 1.40$ mT is due to the presence of small quantities of Ba(Φ_I) or to the existence of another BLA phase with β-type mirror planes of Φ_I type. Studies on powders with compositions $x < 1.2$ are necessary to determine the nature of the phase containing the Φ_I-type F^+ center.

(V) Conclusions

We used X-ray-induced F^+ centers to identify β-alumina-type mirror planes in barium hexaaluminate (Ba(Φ_I) and Ba(Φ_{II})) and in barium–lanthanum hexaaluminate (BLA) phases. The following conclusions can be drawn from this work:

(i) Ba(Φ_{II}) possesses only one type of mirror plane containing defect oxygen ions, and the barium content of these planes seems to be lower than that in Ba(Φ_I). These findings suggest that the F^+ center in Ba(Φ_{II}) lies in "defect mirror planes" similar to those proposed in the models of Iyi *et al.* (*9, 10*) (for BaPb(Φ_{II})) and of Wagner and O'Keeffe (*15*) (for barium hexagallate phase II).

(ii) For BLA compound, we confirm the hypothesis of a segregation of Ba^{2+} and La^{3+} in different mirror planes of β- and MP-types, respectively.

(iii) The structure of β-alumina-type mirror planes of BLA ($x > 1.3$) is very similar to that of the defect mirror planes of Ba(Φ_{II}).

References

1. For a recent review, see R. Collongues, D. Gourier, A. Kahn, J. P. Boilot, and Ph. Colomban, *J. Phys. Chem. Solids* **45,** 985 (1984) and references therein.
2. R. C. Ropp and B. Caroll, *J. Amer. Ceram. Soc.* **63,** 416 (1980); J. M. P. Verstegen, J. L. Sommerdijk, and J. L. Verriet, *J. Lumin.* **6,** 425 (1973); A. Kahn, A. M. Lejus, M. Madsac, J. Thery, D. Vivien, and J. C. Bernier, *J. Appl. Phys.* **52,** 6864 (1981).
3. K. Kato and H. Saalfeld, *Neues Jahrb. Mineral Abh.* **109**(3), 192 (1968); A. J. Lindop, C. Matthews, and D. W. Goodwin, *Acta. Crystallogr. Sect. B* **31,** 2940 (1975).
4. F. Haberey, G. Oehlschlegel, and K. Sahl, *Ber. Dtsch. Keram. Ges.* **54,** 373 (1977).
5. S. Kimura, E. Bannai, and I. Shindo, *Mater. Res. Bull.* **17,** 209 (1982).
6. N. Iyi, Z. Inoue, S. Takekawa, and S. Kimura, *J. Solid State Chem.* **52,** 66 (1984).
7. F. P. F. van Berkel, H. W. Zandbergen, G. C. Verschoor, and D. J. W. Ijdo, *Acta Crystallogr. Sect. C* **40,** 1124 (1984).
8. N. Iyi, S. Takekawa, Y. Bando, and S. Kimura, *J. Solid State Chem.* **47,** 34 (1983).

9. N. IYI, Z. INOUE, S. TAKEKAWA, AND S. KIMURA, *J. Solid State Chem.* **60,** 41 (1985).
10. N. IYI, Y. BANDO, S. TAKEKAWA, Y. KITAMI, AND S. KIMURA, *J. Solid State Chem.* **64,** 220 (1986).
11. P. E. D. MORGAN AND T. M. SHAW, *Mater. Res. Bull.* **18,** 539 (1983).
12. N. YAMAMOTO AND M. O'KEEFFE, *Acta Crystallogr. Sect. B* **40,** 21 (1984).
13. H. W. ZANDBERGEN, F. C. MIJLHOFF, D. J. W. IJDO, AND G. VAN TENDELOO, *Mater. Res. Bull.* **19,** 1443 (1984).
14. A. L. N. STEVELS, *J. Lumin.* **17,** 121 (1978).
15. T. R. WAGNER AND M. O'KEEFFE, *J. Solid State Chem.* **73,** 19 (1988).
16. T. GBEHI, J. THERY, AND D. VIVIEN, *Mater. Res. Bull.* **22,** 121 (1987).
17. A. KAHN AND J. THERY, *J. Solid State Chem.* **64,** 102 (1986).
18. K. O'DONNELL, R. C. BARKLIE, AND B. HENDERSON, *J. Phys. C* **11,** 3871 (1978).
19. D. GOURIER, D. VIVIEN, AND J. LIVAGE, *Phys. Status Solidi A* **56,** 247 (1979).
20. S. R. KURTZ, D. G. STINSON, AND H. J. STAPLETON, *Phys. Rev. B* **24,** 4983 (1981).
21. D. GOURIER, T. GBEHI, R. VISOCEKAS, J. THERY, AND D. VIVIEN, *Phy. Status Solidi B* **152,** 415 (1989).
22. D. GOURIER, F. LAVILLE, D. VIVIEN, AND C. VALLADAS, *J. Solid State Chem.* **61,** 67 (1986).
23. T. GBEHI, PhD thesis, Paris (1987).
24. A. KAHN, T. GBEHI, J. THERY, AND J. J. LEGENDRE, *J. Solid State Chem.* **74,** 295 (1988).
25. P. R. MORAN, S. H. CHRISTENSEN, AND R. H. SILSBEE, *Phys. Rev.* **124,** 442 (1961).
26. R. C. BARKLIE, J. R. NIKLAS, J. M. SPAETH, AND R. H. BARTRAM, *J. Phys. C* **16,** 579 (1983).
27. D. GOURIER, unpublished results.
28. B. S. GOURARY AND F. J. ADRIAN, *Phys. Rev.* **105,** 1180 (1957).
29. J. J. MARKHAM, *Solid State Phys. Suppl.* **8,** 326 (1966).
30. See, for example, J. P. BOILOT, PH. COLOMBAN, AND R. COMES, *Solid State Ionics* **5,** 157 (1981) AND Y. LE CARS, PhD thesis, Paris (1974).